Monitoring of a dust explosion in a 10 m3 vessel

Yann Gregoire, Christophe Proust, Emmanuel Leprette, Didier Jamois

Monitoring of a dust explosion in a 10 m³ vessel

Yann Grégoire [a], Christophe Proust [a,b], Emmanuel Leprette [a], Didier Jamois [a]

[a] : INERIS, Verneuil-en-Halatte, France

[b] : UTC, Compiègne, France

1   Introduction

To mitigate the effects of an industrial dust explosion, various explosion mitigation systems may be used (vent panels, explosion suppressing systems, …) [1]. Those need to be certified as dust explosion protection devices according to the ATEX directive and the certification is based on the experimental demonstration of their efficiency. However, such demonstration has to be performed in specific condition that must be representative of their intended use. Today, no standardized procedure exists for generating an explosive dust could in explosion volumes larger than 1 m³. Furthermore, large variations due to a scale effect have already been identified between the standardized test in the 20 l Siwek sphere or the ISO6184 1 m³ vessel [2]. However industrial installations are often composed of several enclosures of much wider capacities and the generation of controlled large scale dust explosions is a complicated problem. In this paper we aim to present some of the latest works performed at INERIS in view of generating controlled dust explosions in a 10 m³ volume and getting a better understanding on the dust flame behavior in such conditions.

Figure 1. Explosion in a 10 m³ vessel with a transparent face

2   Experimental setup

To ease the understanding of the mechanisms at stake, a parallelogram shaped vessel, with a transparent front face, with a cross section of about 1,5 x 1,5 m and a length of 4 m was built (Fig. 1).

Figure 2. 10 m^3 vessel with a transparent face

Organic dust (wheat flour, cornstarch, …) are often selected as fuel in INERIS applications. Those are injected into the vessel with a specifically designed injector based on fluidized particle bed technique (visible on the right side in Fig. 2). Details concerning the dust injector are not intended in the present study, but one can summarize its functioning: it is made of a transparent 70 l cylinder pressurized up to 10 bar during the dust injection (after a particle-air mixing phase), which is performed within about 10 seconds through a DN45 pipe. The dust is injected at center of the right wall of the confinement. Most of the tests consisted in monitoring the dust injection without ignition of the cloud to measure the dust cloud repartition, concentration and turbulence. Controlling those three parameters is a fundamental for the generation of reproducible explosions. To achieve this goal, measurements are performed at two scales: a local scale, through the "classical" use of sensors placed at various locations of interest, and a global scale where innovative image processing algorithms are used on the complete video sequences of the dust injection. The local sensors consist in three turbulence gauges and three opacimeters placed at about mid-range in height between the central axis of the vessel and its roof, at the both ends (right and left, 40 cm from the walls) and the middle of the structure. Also a pressure gauge is placed in the dust injector. Alternatively, the global scale measurement consists in optical flow computation and analysis on the cinematographic records of the events (Photron high speed camera at 500 images/s in a 1024 x 464 pixels² window). Explosion tests were also performed (see Fig. 1). In such case, the wall at the left side of the confinement (Fig. 2) was replaced by an inertialess plastic foil (opening when the explosion overpressure exceeds 50 mbar). The ignition of the reactive mixture is performed with 2 5 kJ chemical igniters (similarly as the standard 1 m^3 vessel case).

3   Phenomenology of the generation of the dust cloud

A complete description of the phenomenology is out of the scope of the present abstract. The present discussion is limited to specific features of the cloud development that are helpful for the understanding of the following parts of this study. The dust dispersion can be summarized with the following schematic:
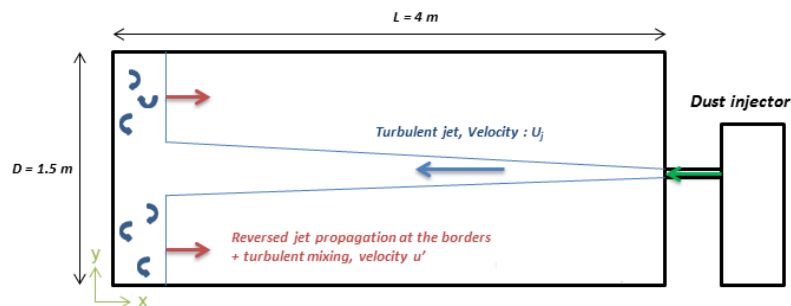

Figure 3. Schematic of the dust cloud formation in the 10 m^3 vessel

The cloud formation in the confinement can be summarized as follows: first the combustible mixture is injected at a high velocity ($\approx$ 240 m/s). A conical turbulent jet is formed, and impacts the left wall. The mixture moves then towards the right side at a lower entrainment velocity close to 10 m/s. Assuming the highly turbulent jet spread with a half angle of 11.8° [3], one can evaluate the delay to cover the whole volume of the vessel: 1,25 s. As observed in the cinematic records, the whole 10 m^3 volume is covered within 1,3 s. Such eye-measurement is inaccurate but the result remains consistent with the jet theory. In the meantime, turbulent structures of intensity u' are induced by the reverse movement of the jet and its interaction with the walls, they are expected to homogenize the local turbulence and dust concentration fields. To evaluate the turbulence intensity u' and scale L_t, it is possible to use the free jets models from Hinze [4]. In the present configuration, the maximal u' velocity should be close to 7 m/s (similarly the integral scale of the turbulence L_t is close to 130 mm, see [5] for further details on the calculation). It is expected to fall down to 1 m/s within 7 s. This model usually provides results in good accordance with experiments, it has also been compared with other experiments performed at INERIS and published in the scientific literature [6]. At last, with the current dimensions of our system, and the injection pressure, it is estimated that the diffusion time over the whole volume, by the turbulence only would be on the order of 10 s which is comparable to the total time of the complete dust injection. Our objective is to obtain a homogeneous cloud in terms of dust concentration but also with a minimal local turbulence intensity to ensure most of the particles remain in suspension (the sedimentation velocity is expected to be close to 1 m/s in the present case). Note that knowing the turbulence parameters u' and L_t, it is possible to estimate the turbulent combustion velocity St of the dust with models available in the literature, such as Gülder's model [7] (details on the application of the model to large dust cloud are available in [8]).

4   Local turbulence and concentration measurements

Measuring the turbulence in a dust air mixture is subject to serious difficulties as the application of standard laboratory equipment's such as LDA or hot wire anemometry may be challenging. INERIS has been working for years on the development of alternative techniques [9]. A Pitot tube technique based on a very refined concept of Mc Caffrey gauges [10] was implemented. Extensive testing in a reference jet proved that such transducers are able to detect eddies as small as 2 cm with a peripheral velocity of 0,2 m/s. Note in particular that the devices can do measurements even in very dusty mixtures (up to 500 g/m^3 at least). Tests were performed in several conditions of dust concentration from 0 to 500 g/m^3. Typical records are compared with the optical flow method in paragraph 5.

To support flame propagation, a sufficient fuel concentration is needed. In the present case the fuel consists in dispersed particles of micrometric dimensions (of grain size distribution comprised typically between 10 and 100 µm, roughly spherical) of organic material. INERIS worked extensively on concentration measurements in dust clouds over the past 10 years [9]. Our sensors are typically made of light source and a receptor separated by a few tenth of mm. Several devices were tested for the light source (laser, LED) as well as for the receptor (photodiodes, solar panels, …) but also the material of the diaphragms of the systems (aluminum, Teflon), chosen to prevent dust accumulation. A major issue is that the high dust concentration levels (>200 g/m^3) in the highly turbulent cloud quickly cloaks the system, making the measurement impossible. To overcome the dust accumulation problem, a cell-phone buzzer was added in the device. Results are promising as even in a very dense dust cloud (4 kg/ m^3), the receptor blank level (no dust between the light source and the receptor) change by less than 10 % between before and after the experiment. Another issue that we were confronted to is the limitations of the original Beer-Lambert absorbance law which supposes an extinction coefficient that only depends on the wavelength. However, it is very likely that the micrometric particles will diffuse the light differently as a function of their diameter, thus changing

the light intensity on the receptor. A theoretical model was proposed by Proust [9] to take this phenomenon into account:

$$\tau = \mathrm{Ln}\left(\frac{I_0}{I_{(x)}}\right) = \frac{3}{2} \times \frac{Q_{ext} \times \sigma}{\delta \times \rho} \times x \tag{1}$$

where I_0 is the reference light intensity, I the light intensity on the receptor when the light ray passes through a dust cloud of thickness x, Q_{ext} an extinction coefficient (close to 2 [9]), σ the dust concentration, ρ the thermodynamic density of the particles and δ their diameter. The system was calibrated using laser granulometry, right next to the opacimeter. Note that a quick dimensional analysis on equation (1) shows the physics behind the model: the absorbance remains proportional to the effective absorption area. At last some measurements are performed in the 10 m³ vessel. An example is provided in Fig. 4:
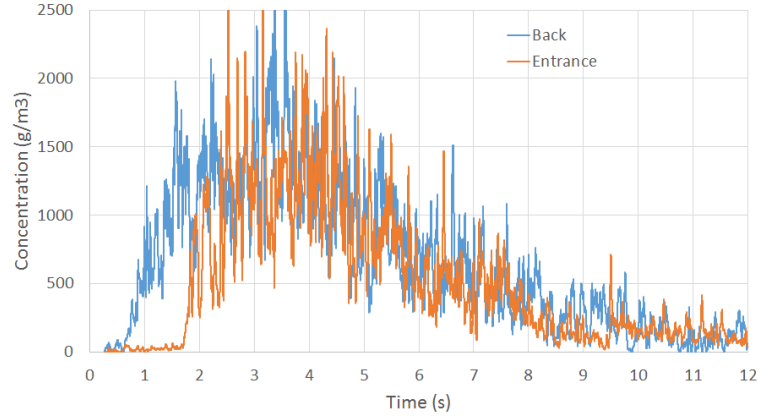

Figure 4. Concentration measurements at the back and entrance of the 10 m³ vessel

Such measurement is still relatively inaccurate but it gives a satisfying order of magnitude of the local dust concentrations. These sensors are currently being miniaturized to limit their effect on the dust flow.

5- Global flow measurements through optical flow computation

The concept of Optical Flow was introduced by a psychologist, Gibson in 1950 [11] as a description of the movement perception. Robust algorithms to measure it, emerged in the beginning 1980's. These algorithms, based on differential methods, proposed by Horn-Schunck [12] and Kanade-Lucas [13] are now at the basis of most of the more recent algorithms. Optical flow is widely used for motion estimation (mostly in robotics and computer vision) and in video compression. To our knowledge it is progressively being transferred to other domains such as fluid mechanics: however, most research articles related to this topic are entirely focused on the optical flow computation algorithm or its performances (robustness to noise, accuracy) rather than the actual analysis of the physics behind the results obtained (see for example[14]). Several optical flow algorithms exist, the one we selected for the present is an improved Horn-Schunck formulation based on the works of Sun [15]. The measurement has some limitations such as it is limited in the front plane of the vessel, or it shows poor performance in the presence of noise or occlusions. However, the code computes the velocity field between 2 images over the whole video, and provides, non-intrusively, for each pixel of each of the images, the velocity vector coordinates. Such calculation is quite demanding as we work on more than 3000 pictures of 1024 x 464 pixels and for each image the optimized yet complex algorithm has to solve several linear systems of up to 950000 equations. We believe it is one of the reasons why such algorithms were barely used until now in fields other than computer science.

Direct comparison between the macroscopic velocities (i.e. front velocities of the jet) found by the optical flow method and a rough measurement on the video gave similar results. Because this method was used for the first time, our first attempt was to ensure its results were in good agreement with the course of the experiment. Secondly it has been decided to compare the velocities measured by our Pitot turbulence sensors (see paragraph 4) with the velocity field in the close surrounding of the sensors (Fig 5, left):
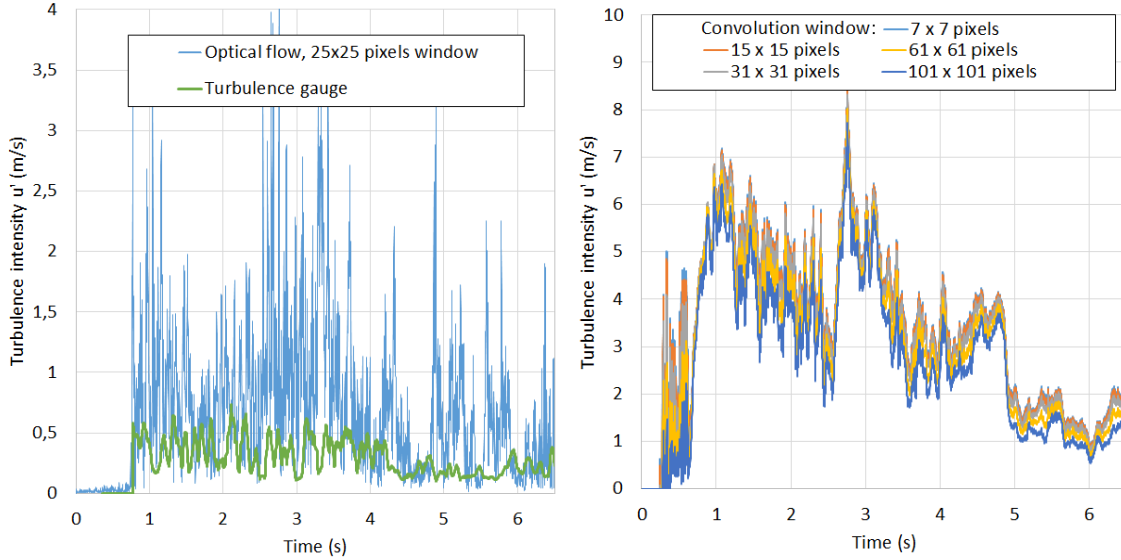

Figure 5. Left: Optical flow calculation of the turbulence intensity in the vicinity of a turbulence gauge compared with the gauge measurements. Right: Turbulence intensity estimated in the whole domain with the optical flow method and variable convolution windows

Here again the agreement is satisfying as the same order of magnitude is found for the sensors and the optical flow method (note that the flow measurement is performed in the plane surface located at 75 cm before the turbulence gauge, so higher values of the velocity were expected). At last an interesting feature of the optical flow measurements was exploited. It is the dense nature of the results, which provide a large number of velocities over each image. This was used to compute statistically the standard deviation of the velocity field through multiple convolution products of the velocity matrix with square windows between 7 and 101 pixels² (see Fig. 5, right). The standard deviation of the local velocity field represents the turbulence intensity [4]. Here the same order of magnitude as estimated in paragraph 3 with the phenomenological analysis is found (7 m/s). Further evolutions of the overall turbulence in the vessel can be tracked with an acceptable accuracy, showing a drastic fall of the turbulent velocities after 5 s. Consequently, this tool seems very promising for the statistical turbulence analysis. Next steps of the study will include tentative of measuring the integral scale of the turbulence through optical flow calculation.

6   Further developments

Measuring the turbulence intensity and scale, as well as the dust concentration is helpful to determine when and where the cloud can be ignited. In the present example (with 500 g/m³ of wheat flour), ignition is performed in the jet close to the injection location, 5 s after the beginning of the dust injection. In those conditions the dust concentration and turbulence cannot fully diffuse and homogenize through the whole volume. Also there is a pressure gradient due to the jet, but this is the best compromise so far to prevent the

sedimentation of the dust. A possible solution to this problem would thus be to a have two injectors rather than this single one or an additional flow mixing device in the vessel. The transparent face is also of a great help to analyze the flame behavior: a conical flame development is observed, it grows until it reaches the left wall, then goes backwards despite the vent opening, following the dominant flow velocities of the unburnt material. Optical flow analysis will also be performed on these tests, in view of characterizing numerically the flame growth and velocity. Implementing this flame surface growth in INERIS phenomenological tool EFFEX for confined explosion [16], make it possible to model the explosion with an increased accuracy. At later time explosions performed in this vessel with a transparent face with different kinds of particles will also aim to select the best test parameters (ignition delay, injection pressure) before testing of protective equipment in imposed conditions of dust nature or concentration, K_{ST}, ...

References

[1] Eckhoff R.K., (2003), Dust Explosions in the Process Industries (Thrid Edition), ISBN: 9780750676021

[2] Proust C., Accorsi A., Dupont L., (2007), Measuring the violence of dust explosions with the ''20 l sphere'' and with the standard ''ISO 1m^3 vessel'' Systematic comparison and analysis of the discrepancies, Journal of Loss Prevention in the Process Industries 20 599–606

[3] Turner J.S., (1986), Turbulent entrainment: the development of the entrainment assumption, and its application to geophysical flows, Journal of Fluid Mechanics, vol. 173, pp. 431-471.

[4] Hinze J.O., (1975), Turbulence, 2nd edition, Mc Graw-Hill company, New-York, ISBN 0070290377

[5] Proust C., Daubech J., Leprette E., (2009), Differentiated routes for the simulation of the consequences of explosions, Journal of Loss Prevention in the Process Industries, Volume 22, Issue 3, Pages 288–294

[6] Roux P., Proust C., (1999), "Adaptation, extension et promotion de la norme NFU54-540 de décembre 1986, rapport final pour le compte du Ministère de l'Industrie-SQUALPI, convention n° 96 2400051.

[7] Gülder Ö.L., (1990), Turbulent premixed flame propagation models for different combustion regimes, Proceedings of The Combustion Institute, Vol.23, pp.743–750.

[8] Proust C., (2016), Turbulent Flame Propagation in large Dust Clouds, 11th ISHPMIE, Dalian, China

[9] Proust Ch. (2004), « Formation, inflammation, combustion des atmospheres explosives (ATEX) et effets associés », Mémoire d'HdR présenté à l'Institut National Polytechnique de Lorraine, 12 Fév 2004

[10] Mc Caffrey, B.J. and Heskestad, G. (1976). A robust bidirectional low-velocity probe for flame and fire application, Comb. and Flame, 26, 125.

[11] Gibson, J.J. (1950). The Perception of the Visual World. Boston: Houghton Mifflin

[12] Horn B.K., Schunck B.G., (1981), Determinig optical flow, Artificial Intelligence, vol 17, pp 185–203

[13] Lucas B. D. and Kanade T. (1981), An iterative image registration technique with an application to stereo vision. Proceedings of Imaging Understanding Workshop, pages 121—130

[14] Heitz D., Heas P., Navaza V., Carlier J., Memin E. (2007), Spatio-temporal correlation-variational approach for robust optical flow estimation, 7th International Symposium on Particle Image Velocimetry

[15] Sun D., Roth S., Black M.J., (2014), A quantitative analysis of current practices in optical flow estimation and the principles behind them, Int. J. Comput. Vis., 106 (2), pp. 115-137.

[16] Proust. C., (2004), EFFEX: a tool to model the consequences of dust explosions. 11th International Symposium on Loss Prevention and Safety Promotion in the Process Industry, Praha, Czech Republic